


ORIGINAL ARTICLE

The effect of cannabidiol on canine neoplastic cell proliferation and mitogen-activated protein kinase activation during autophagy and apoptosis

Joshua G. Henry¹ | Gregory Shoemaker² | Jennifer M. Prieto¹ |
Many Beth Hannon¹ | Joseph J. Wakshlag¹ 

¹Department of Clinical Sciences, Cornell University College of Veterinary Medicine, Ithaca, New York

²Comparative, Diagnostic, Population Medicine, University of Florida College of Veterinary Medicine, Gainesville, Florida

Correspondence

Joseph J. Wakshlag, Department of Clinical Sciences, Cornell University College of Veterinary Medicine, Veterinary Medical Center C2-009, Ithaca, NY 14853, USA.
Email: jw37@cornell.edu

Funding information

American Kennel Club Canine Health Foundation, Grant/Award Number: 02643-A

Abstract

Low tetrahydrocannabinol *Cannabis sativa* products, also known as hemp products, have become widely available and their use in veterinary patients has become increasingly popular. Despite prevalence of use, the veterinary literature is lacking and evidence-based resource for cannabinoid efficacy. The most prevailing cannabinoid found in hemp is cannabidiolic acid (CBDA) and becomes cannabidiol (CBD) during heat extraction; CBD has been studied for its direct anti-neoplastic properties alone and in combination with standard cancer therapies, yielding encouraging results. The objectives of our study were to explore the anti-proliferative and cell death response associated with in vitro treatment of canine cancer cell lines with CBD alone and combination with common chemotherapeutics, as well as investigation into major proliferative pathways (eg, p38, JNK, AKT and mTOR) potentially involved in the response to treatment with CBD. CBD significantly reduced canine cancer cell proliferation far better than CBDA across five canine neoplastic cell lines when treated with concentrations ranging from 2.5 to 10 µg/mL. Combinatory treatment with CBD and vincristine reduced cell proliferation in a synergistic or additive manner at anti-proliferative concentrations with less clear results using doxorubicin in combination with CBD. The cellular signalling effects of CBD treatment, showed that autophagy supervened induction of apoptosis and may be related to prompt induction of ERK and JNK phosphorylation prior to autophagy. In conclusion, CBD is effective at hindering cell proliferation and induction of autophagy and apoptosis rapidly across neoplastic cell lines and further clinical trials are needed to understand its efficacy and interactions with traditional chemotherapy.

KEYWORDS

annexin, cannabinoid, caspase, chemotherapy, LC3, SQSTM1/p62, synergy

1 | INTRODUCTION

The use of *Cannabis sativa* is reported throughout history for its medicinal uses dating back to 2900 BC in the writings of Chinese Emperors.¹ Although the use of *C. sativa* spans several millennia,

formal scientific exploration of its clinical applications is in its infancy. In 1964, the primary psychoactive cannabinoid in *C. sativa*, Δ9-tetrahydrocannabinol (THC), was discovered.² Decades later, the first endogenous G-protein-coupled receptor (GPCR), cannabinoid receptor 1 (CB1), was identified.^{3,4} Since these discoveries, our

understanding of the endocannabinoid system has continued to grow through the recognition of the primary endogenous ligands including the fatty acid derivatives *N*-arachidonylethanolamine (anandamide) and 2-arachidonoylglycerol (2-AG), resulting in an expanded understanding of their endogenous targets for cannabinoids including orphan GPCRs, transient receptor potential cation channels (TRPVs) and peroxisome proliferation receptors (PPARs).⁵⁻⁹

Considering the illegal nature of THC, because of the psychotropic properties, there has been accelerated interest in other cannabinoids, namely cannabidiol (CBD). Cannabinoids (eg, dronabinol) have been studied and utilized for the palliation of cancer symptoms or for the treatment of side effects related to standard cancer therapies.¹⁰⁻¹²

However, more recent studies have been exploring CBD and its direct antineoplastic properties alone or in combination with standard cancer therapies, such as chemotherapy or ionizing radiation.¹³⁻¹⁶ Equally, if not more interesting, is the ability for CBD to activate GPCR18, and GPCR55 whose actions are poorly elucidated in cancer cell biology,^{17,18} but appear to control ion channels or incite activation of signalling cascades.^{19,20}

Glioblastoma multiforme has been a major focus of cannabinoid-based research in human tumour models. These studies have demonstrated a reduction in the cell viability of glioma cell lines treated with CBD, as well as synergetic reductions in cell viability in combination with ionizing radiation and/or DNA-damaging agents both in vitro and in xenograft murine models.^{14,15,21} Induction of apoptosis has been observed in many cell culture models and there appear to be numerous cell signalling pathways affected leading to apoptosis and/or autophagy, namely the mammalian target of rapamycin (mTOR), phosphatidylinositol-3 kinase (PI3K) and mitogen-activated protein (MAP) kinases.²²⁻²⁶ To date, there has been little to no examination of the effects of CBD on canine cell culture models or the effects of standard CBD-rich hemp extracts.

The use of hemp extracts in controlling cellular growth is exceedingly complex considering hemp extracts with relatively similar CBD concentrations appear to have differential effects on cell culture systems leading to the proposition of the “entourage effect” whereby terpenes and other cannabinoids may be acting synergistically with CBD to influence cell proliferation.²⁷⁻²⁹ More importantly, we need to better understand the cell death response in conjunction with chemotherapeutic agents commonly used in veterinary treatment, as many owners want to utilize CBD-rich hemp products during chemotherapy for the effects on the cancer itself, or to relieve some the adverse effects of chemotherapy (nausea and lethargy) to maintain or improve their pet's quality of life.³⁰

We set out to examine the effects of CBD and a CBD-rich hemp extract treatment on 5 different canine cell culture systems (3 osteosarcoma, 1 mammary carcinoma and 1 lymphoma). The objective of our study was 3-fold; (a) to better understand the anti-proliferative and cell death response associated with CBD through induction of apoptosis and/or autophagy, (b) to understand combination index (CI) synergy or antagonism utilizing doxorubicin or vincristine in combination with CBD treatment, and (c) to examine the major cell signalling pathways involved in cellular proliferation including the

extracellular regulated kinase (ERK), p38 mitogen activated kinase (p38), janus/kinase activation (JNK), protein kinase B (AKT) and mechanistic target of rapamycin (mTOR) pathway induction when treating neoplastic cell lines with CBD.

2 | MATERIAL AND METHODS

2.1 | Cannabinoids and chemotherapeutics

CBD and its acid derivative CBDA were purchased as a 10 mg/mL and a 1 mg/mL formulation in methanol, respectively (Cayman Chemical Corporation, Ann Arbor, Michigan). A whole hemp based extract was received directly from a manufacturer with third party analysis (Proverde Laboratory, Milford, Massachusetts) revealing a product with approximately 30 mg/mL of CBD, 31 mg/mL CBDA, 1.4 mg/mL THC and 1.3 mg/mL tetrahydrocannabinolic acid (THCA) with less than 1 mg/mL of cannabigerol, cannabichromene and cannabinol, and 5.2 mg/mL of complex terpenes (ElleVet Sciences, Portland, Maine) in an ethanol base. The extract was diluted to a 20 mg/mL in a 50%/50% mix of ethanol and DMSO. The final stock extract contained 20 mg/mL of cannabidiols as an equal mix of CBD (10 mg) and CBDA (10 mg) as well as 0.4 mg/mL THC, 0.4 mg THCA, 0.1 mg or less of cannabichromene (CBC) and cannabigerol (CBG) with 1.8 mg of complex terpenes. Chemotherapeutic agent doxorubicin hydrochloride (Sigma Aldrich, St. Louis, Missouri) was freshly diluted in water to a 2 mM stock solution, while vincristine sulfate (Sigma Aldrich, St. Louis, Missouri) was prepared as a stock solution of 10 µM in sterile water before utilizing in cell culture experiments.

2.2 | Cell lines and culture conditions

Five established canine neoplastic cell lines were obtained and used for all experiments; a cell line of epithelial mammary gland carcinoma cell line—CMT12 (provided by Dr Curtis Byrd), a B cell lymphoma lineage—17-71 (provided by Dr Angela Wheeler), and three mesenchymal osteosarcoma lines HMPOS (provided by Dr Rodney Page), D17 (#CCL-183; ATCC, Manassas, Virginia) and Abrams (provided by Dr Angela Wheeler). The Abrams cell line was validated from its original source, while the D17 cell line is a validated cell line from the American Type Culture collections. The CMT12, 17-71 and HMPOS cell lines have not been validated genetically but display cell markers and characteristics of epithelial, round and osteosarcoma cell lines, respectively. All cell lines were deemed mycoplasma free by polymerase chain reaction from the Animal Health and Diagnostic Laboratory at Cornell University.

All cells were maintained on tissue culture-treated plates (Laboratory Product Sales [LPS], Rochester, New York) with Roswell Park Memorial Institute (RPMI) medium 1640 (Invitrogen, Carlsbad, California) with 10% fetal bovine serum (FBS; Invitrogen, Carlsbad, California) and 1% antibiotic and antimycotic solution (Invitrogen, Carlsbad, California). Cell lines were grown at 37°C and 5% CO₂ for all

experiments and passage of cells, unless indicated otherwise. Canine primary dermal fibroblast (Applied Biological Materials [ABM], Richmond, BC, Canada) were propagated and kept on PriCoat T25 flasks (ABM) in Prigrow II medium (ABM) containing 10 HI-FBS and 1% penicillin/streptomycin (Invitrogen, Carlsbad, California). The dermal fibroblasts were used to determine the effects of the extract on normal cells.

2.3 | Cannabidiols and CBD-rich hemp 48 hours MTT proliferation

3-(4,5-Dimethylthiazol-2-yl)-2,5-diphenyltetrazolium bromide (MTT) assays were performed on all previously described cell lines; CMT12, HMPOS, D17, Abrams and 17-71. Cells were plated at a density of 2500 cells per well in 96-well tissue culture-treated plates (Laboratory Product Sales, Rochester, New York). Cells were treated with vehicle (methanol or ethanol/DMSO mix) or various concentrations of the CBD, CBDA or CBD-rich hemp extract ranging from 0.42 to 20 µg/mL in serial dilution for 48 hours. MTT assays were performed after 48 hours of treatment by adding 20 µL of MTT dye (0.7 µM filtered 5 mg/mL in phosphate-buffered saline [PBS]) to each well and incubating at 37°C in 5% CO₂ for 2 hours. The media was then aspirated, washed once with 200 µL of PBS and then solubilized in 200 µL of ethanol. Immediate analysis of the optical density of each well was performed using a spectrophotometric plate reader (Epoch; Biotek, Winooski, Vermont) at a wavelength of 570 nm as previously described.³¹ The percent proliferating cells of control for each concentration was averaged and reported as a mean ±SD from triplicate wells over three experiments.

2.4 | Doxorubicin cytotoxicity/proliferation assays

CMT12, 17-71 and D17 cells were plated at a density of 2500 cells per well in 96-well tissue culture-treated plates (Laboratory Product Sales, Rochester, New York). All cell lines were treated with identical concentrations of the pure CBD (0.34, 0.67, 1.25, 2.5, 5, 10, 20 g/mL) and various concentrations of doxorubicin or vincristine. The concentration of doxorubicin varied between cell lines in order to achieve between 20% and 80% proliferation inhibition. The cell lines were treated with serial dilutions of doxorubicin as follows; CMT12 and D17 (0.067–2 µM) and 17-71 (0.0167–0.5 µM). Methanol was used as a vehicle control for all CBD treatments and sterile water for doxorubicin and vincristine at the highest doses used to represent the vehicle control treated wells. Cells were then incubated for 48 hours prior to performing MTT assays, as previously described. Wells treated with the vehicle control were considered to represent 100% proliferating cells in triplicate over three experiments. Percent viable cells for each specific combination were averaged and reported as mean percent proliferation ±SD for further CI evaluation.

2.5 | Trypan blue exclusion assay of cell viability

The trypan blue exclusion assay was performed on canine primary dermal fibroblasts (CDF) because of the slow rate of proliferation and low metabolic activity of these normal canine cells, precluding productive MTT assays. The effects of CBD treatments were compared with the results obtained on the 17-71, CMT12 and D17 cell lines for comparative purposes. For the CDF cells, applied cell extracellular matrix (ABM) was applied overnight to 24-well tissue culture-treated plates (Applied Biological Materials [ABM], Richmond, BC, Canada). For all cell lines, cells were plated at a density of 5×10^3 cells per well and incubated until 60% confluent before treatment with methanol vehicle control, 3.75, 7.5, and 15 µg/mL of CBD to cells for 48 hours. Cells were then trypsinized, collected and centrifuged at 1900 g for 10 minutes. With the exception of the 17-71 cell line, cells were detached with Accumax (Invitrogen, Carlsbad, California). The cell pellet was resuspended in 0.1% trypan blue (Sigma Aldrich, St Louis, Missouri) in PBS solution, loaded on a Cell Countess disposable cell counting slide with automatic counting of all positively stained cells in the Countess II Cell Counter under identical settings for each cell line (Invitrogen; ThermoFisher Scientific, Carlsbad, California) using the same parameters for each cell line. All treatments were performed in triplicate and the percent of viable cells were averaged.

2.6 | MTT and trypan blue data management and calculations

Raw data from MTT proliferation assays and trypan blue exclusion assays (individual optical density of each well) were normalized to the vehicle control treatment for each cell line, considered to represent 100% proliferating cells (single or combined treatment). The percent proliferating cells was determined by comparing optical density readings or live counts, respectively, of treatment wells at each concentration compared with vehicle control wells in each cell line.

For CBD, CBDA and hemp extract concentrations needed to obtain a 50% inhibition of cell proliferation (IC₅₀) were then calculated across experiments by Probit analysis using XLFit5 software (IDBS, Guildford, United Kingdom) for reporting the results for each cell line.

The compound interactions of chemotherapy and CBD treatment in the CI studies were calculated by multiple drug effect analysis using Compusyn software (v.2; Compusyn Inc, Paramus, New Jersey) which employs the median equation principle according to the methodology described by Chou and Talalay to determine a CI value by the formula³²:

$$CI = \frac{(D)_1}{(D_x)_1} + \frac{(D)_2}{(D_x)_2} + \frac{(D)_1(D)_2}{(D_x)_1(D_x)_2}$$

where (D)₁ and (D)₂ are the doses of both compounds in combination and (D_x)₁ and (D_x)₂ are the doses of each compound alone at x percent of inhibition. CI values ≤0.9 indicate synergism, a CI value >0.9 and <1.1 indicates an additive effect, and CI values ≥1.1 indicate antagonism.

2.7 | Annexin V-FITC apoptosis assay

Apoptosis after 4 and 8 hours treatment was measured using Annexin-V staining (Invitrogen Annexin V-FITC staining kit, Carlsbad, California). Briefly, cells were detached with Accumax (Innovative Cell Technologies, San Diego, California), collected and centrifuged for 10 min at 1000 g at 4°C. The pellet was washed once with PBS before resuspension in Annexin Binding Buffer (ABB; 10 mM HEPES, 140 mM NaCl, 2.5 mM CaCl₂, pH 7.4) at a density of approximately 1×10^6 cell/mL. Annexin V-FITC conjugate was added according to the manufacturer's suggestion to the cell suspensions and incubated for 15 minutes at room temperature. After the incubation, ABB was added to the cell suspension and kept on ice until fluorescence was measured with the BD FACScalibur flow cytometer using an argon laser (BD Biosciences, Ashland, Oregon). Ten thousand events were collected per sample. Analysis was performed with the FlowJo software (Version 10.7.1. Becton, Dickinson, Ashland, Oregon) by first gating based on the forward- and side-scatter characteristics for each cell line followed by Annexin V-FITC positive cells. Negative fluorescence controls were unstained cells. Three independent replicates were examined for each treatment.

2.8 | Western blot assessment of signalling pathways and autophagy

Cells were plated on 100 mm tissue culture-treated plates and incubated overnight in complete medium until 60% confluency was reached. Cells were treated with methanol vehicle control or 10 µg/mL of CBD for 2, 4 or 8 hours. Cells were harvested and lysed at each time point for control and CBD treated cells using mammalian lysis buffer (25 mM Tris, 100 mM NaCl, 1 mM EDTA, 1% Triton X-100, pH 7.4), and then centrifuged for 5 minutes at 12 000 g at 4°C. The supernatant was collected and the protein concentration was determined using the Bradford assay (Coomassie-dye; ThermoFisher Scientific Pierce, Waltham, Massachusetts). Samples were equilibrated to a common volume (µg/µL) in lysis buffer and 5× laemmli loading buffer (300 mM Tris-HCl pH 6.8, 10% sodium dodecyl sulfate, 50% glycerol, 12.5% β-mercaptoethanol, 0.025% bromophenol blue). For each protein of interest, 30 µg total protein were subjected to sodium dodecyl sulfate polyacrylamide gel electrophoresis (SDS-PAGE) on gels ranging from 6% to 15% based on the molecular weight of the protein of interest. The proteins were then transferred to 0.45 µm pore size polyvinylidene fluoride membrane (Immobilon-P Membrane, EMD Millipore, Billerica, Massachusetts) for 1 hour at 333 mA and then blocked in 5% milk in tris-buffered saline/0.05% Tween 20 solution (TBST). Membranes were incubated overnight in primary antibody solutions at a dilution of 1:1000 in TBST on a rocking platform at 4°C. Primary antibodies confirmed as cross reactive with canine cells or tissues included mouse extracellular regulated kinase (ERK) (R&D Biosciences, Boston, Massachusetts); rabbit anti- protein kinase B (AKT), Ser473 phosphorylated-AKT, stress-activated protein kinase/jun-amino-terminal kinase (SAPK/JNK), Thr183/Tyr185 phosphorylated-SAPK/JNK, mammalian target of

rapamycin (mTOR), Ser2448 phosphorylated-mTOR, anti-Thr202/Tyr204 phosphorylated p44/42 MAPK (ERK1/2), anti-p38, anti-phosphorylated p38, anti-p62 and anti-LC3 A/B (Cell Signalling Technology, Danvers, Massachusetts).³³⁻³⁶ Membranes were washed three times with TBST and incubated at room temperature for 1 hour in the corresponding secondary anti-rabbit IgG or anti-mouse IgG horseradish peroxidase-conjugated antibody at a dilution of 1:2000 (Cell Signalling Technology, Danvers, MA). Membranes were washed three times with TBST and visualized with a chemi-luminescent reagent (Clarity Western ECL Substrate; Bio-Rad, Hercules, California). Digital images were captured using an imaging system (Biospectrum 410; UVP, Upland, California or FluorChem E; Cell Biosciences, San Jose, California). Each blot was performed twice from two different experiments to confirm findings.

2.9 | D17 and CMT12 immunofluorescence

CMT12 and D17 adherent cell lines were split into Nunc chamber slides (ThermoFisher Scientific, Rochester, New York) and the cells were 70% confluent they were treated for 6 hours with either methanol control or 10 µg/mL of CBD. Cells were fixed with 4% paraformaldehyde for 1 hour and then permeabilized with PBS containing 0.1% Triton X-100 for 30 minutes. Cells were then washed with PBS and incubated with bovine serum albumin (Sigma Aldrich, St. Louis, Missouri) for 30 minutes and then goat anti-serum (Vector Labs, Burlingame, California) for 1 hour and then washed twice with PBS for 10 minutes while rocking at room temperature. Equal concentrations of rabbit polyclonal non-specific antibody (Vector Labs, Burlingame, California) or polyclonal rabbit-anti LC3A/B antibody (Cell Signalling, Danvers, Massachusetts) at identical concentrations as described by Syrja and colleagues.³³ The cells were incubated overnight at 4°C and then washed twice with PBS. Cells were then incubated with a 1:400 dilution of Oregon green 488-conjugated secondary goat anti-rabbit antibody (Invitrogen, Carlsbad, California) for 2 hours at room temperature. Coverslips were mounted using Vectashield DAPI mounting media (Vector Labs, Burlingame, California) and the images were captured at the same fluorescence intensity for each image at 400 or 600 magnification and processed using an Olympus fluorescent microscope and DP controller software (Olympus Corp., Center Valley, Pennsylvania).

2.10 | Statistical analysis

All statistical analysis regarding percent proliferating cells as measured by MTT assay and Annexin-FITC assay were performed using JMP Pro (v. 11.2.1; SAS Institute Inc., Cary, North Carolina). The residuals of the statistical model were evaluated for normality and found to be not normally distributed in most analyses. Therefore, non-parametric Kruskal-Wallis testing was used to compare differences in percent proliferating cells for every treatment dose used within each cell line across experiments. Comparisons between each treatment group and

vehicle control group were carried out using the Steel method adjusting alpha risk for multiple comparisons.

For the outcome of percent viability determined by the trypan blue exclusion assay residuals of the statistical model were found to be normally distributed, and therefore analysed using analysis of variance with Dunnett's method for comparison to vehicle control, controlling for multiple comparisons. Differences were considered statistically significant at $P < .05$ for all statistical testing.

3 | RESULTS

3.1 | 48 hours MTT assays CBD, CBDA and whole hemp extract

When examining the Probit analysis of CBD on the 5 cell lines it was found that the IC_{50} for 17-71 cells was 2.5 $\mu\text{g/mL}$ and the concentrations that caused significantly diminished proliferation were 2.5 $\mu\text{g/mL}$ and above. The CMT12 cell line exhibited a similar profile with significantly diminished proliferation at 2.5 $\mu\text{g/mL}$ and above with a slightly higher probit IC_{50} of 3.5 $\mu\text{g/mL}$. The Abrams, D17 and HMPOS showed similar probit analysis concentrations of 4.1, 4.1 and 3.6 $\mu\text{g/mL}$ respectively, with the concentrations of 5 $\mu\text{g/mL}$ and above being significant for slowing cell proliferation when compared with vehicle control treated cells (Figure 1A).

Whole hemp extract using concentrations of CBD in the extract of 20 $\mu\text{g/mL}$ and lower in conjunction with other cannabinoids and terpenes show that lesser CBD concentrations are needed across all cell lines. The hemp extract showed that the probit IC_{50} was approximately 0.8 $\mu\text{g/mL}$ for the 17-71 cell line, with the first significantly different concentration to slow proliferation being 0.67 $\mu\text{g/mL}$ and higher. CMT12, Abrams, D17, and HMPOS cells probit revealed and IC_{50} 's of 1.5, 1.3, 1.6 and 1.7 $\mu\text{g/mL}$, respectively; and these cell lines showed significant decreases in proliferation at 1.25 $\mu\text{g/mL}$ and higher when compared with vehicle control treated cells (Figure 1B).

Considering the hemp extract used had a significant proportion of CBDA, 48 hours MTT assays were performed with CBDA. CBDA treatment of 17-71 cells exhibited an IC_{50} of 15.1 $\mu\text{g/mL}$, with concentrations of 5 $\mu\text{g/mL}$ and above showing significant slowing of cell proliferation. The CMT12 cell lines showed significant slowing of proliferation starting at 10 $\mu\text{g/mL}$ and higher, and an IC_{50} could not be determined since 50% growth inhibition was not achieved in the assay. The three osteosarcoma cell lines, Abrams, D17 and HMPOS showed significant growth inhibition at 20 $\mu\text{g/mL}$, while IC_{50} calculations could not be calculated because of lack of growth inhibition (Figure 1C).

3.2 | Trypan blue exclusion assay for CBD

The percent trypan blue positive dermal fibroblasts for methanol vehicle control cells were $16 \pm 3\%$ of the cell population. This was

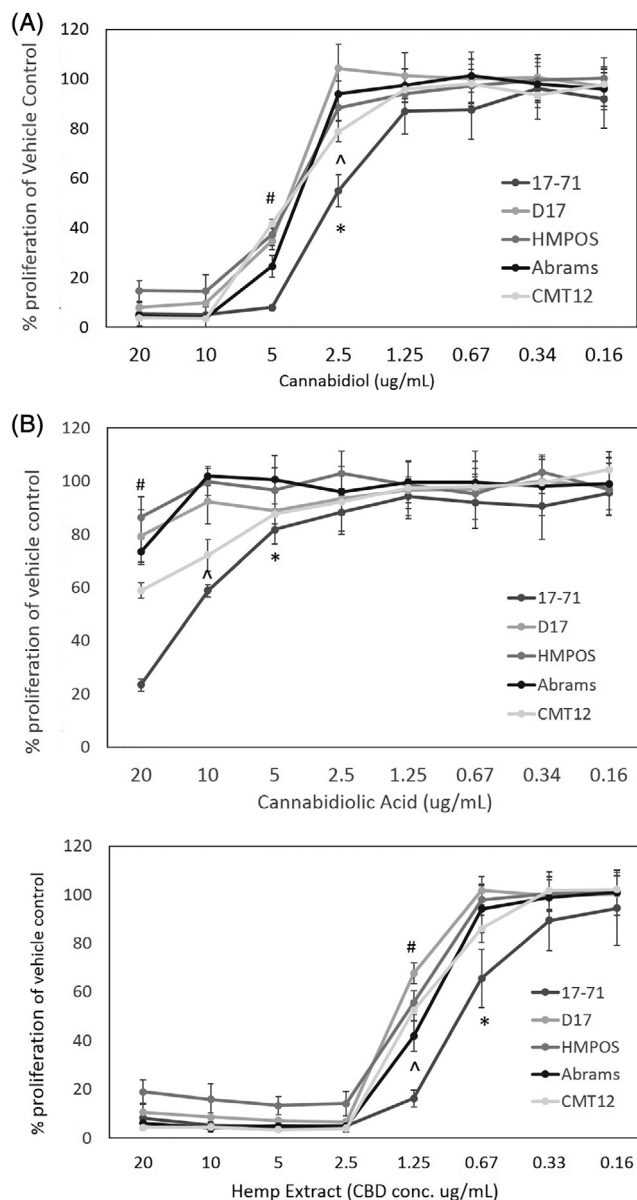


FIGURE 1 Cannabinoid treated 48 hour MTT proliferation assays with mean and standard deviations presented at each concentration. (A) Cannabidiol (CBD); (B) Cannabidiolic acid (CBDA) and (C) CBD-rich whole plant extract. Assays depict assay results on 3 different time points performed in duplicate. * Depicts initial concentration that is significantly different from vehicle control treated baseline for 17-71 including any higher concentrations ($P < .05$). ^ depicts initial point that is significantly different from vehicle control treated baseline for CMT12 including any higher concentrations ($P < .05$). # Depicts initial point that is significantly different from vehicle control treated baseline for D17, HMPOS and Abrams including any higher concentrations ($P < .05$)

significantly higher when treated for 48 hours with 15, 7.5 and 3.75 $\mu\text{g/mL}$ of CBD at $77 \pm 12\%$, $58 \pm 7\%$ and $32 \pm 5\%$, respectively (Figure 2). 17-71 cells showed a $3 \pm 1\%$ trypan blue positive cell population when treated with methanol as vehicle control. There was a significant increase in trypan blue positive cells at both 15 $\mu\text{g/mL}$ and

7.5 $\mu\text{g/mL}$ at $55 \pm 6\%$ and $27 \pm 8\%$, respectively. 17-71 cells treated with 3.75 $\mu\text{g/mL}$ were no different from vehicle control treated cells at $7 \pm 4\%$ positive cells. D17 cells showed a $5 \pm 1\%$ trypan blue positive cell population when treated with methanol as vehicle control. There was a significant increase in trypan blue positive cells at 15 $\mu\text{g/mL}$ at $35 \pm 4\%$. D17 cells treated with 7.5 and 3.75 $\mu\text{g/mL}$ were no different from vehicle control treated cells at $5 \pm 2\%$ and $4 \pm 2\%$ positive cells, respectively. CMT12 cells showed a $3 \pm 1\%$ trypan blue positive cell population when treated with methanol as vehicle control. There was a significant increase in trypan blue positive cells at 15 $\mu\text{g/mL}$ at $87 \pm 8\%$ and 7.5 $\mu\text{g/mL}$ with $9 \pm 3\%$. CMT12 cells treated with 3.75 $\mu\text{g/mL}$ showed no difference from vehicle control treated cells at $4 \pm 2\%$ (Figure 2).

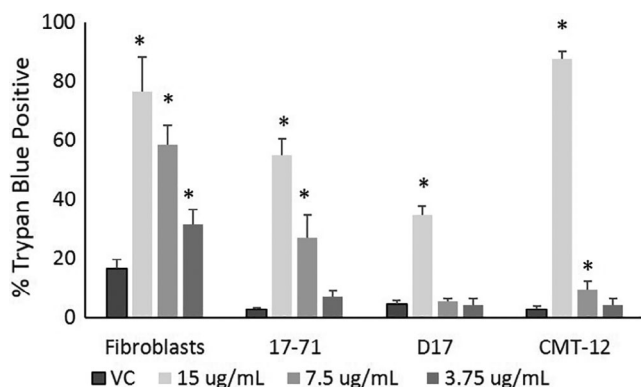


FIGURE 2 Mean and SD percent trypan blue positive fibroblast, 17-71, D17 and CMT12 at 48 after treatment with CBD at 15, 7.5, 3.75 $\mu\text{g/mL}$ and with methanol vehicle control (VC). Each cell line was assessed for trypan positive cell death across three experiments with * indicating a significant increase in trypan positive cells as compared with VC cells ($P < .05$)

3.3 | Combination index MTT dual treatment assays with CBD and chemotherapeutics (doxorubicin/vincristine)

When all three cell lines were treated with doxorubicin the 17-71 lymphoma cell line was most sensitive with inhibitory concentrations from IC_{20} - IC_{80} between 0.033 and 0.125 μM , while CMT12 and D17 cell lines required higher concentrations to hinder cell proliferation (0.5-2 μM). Regardless of the cell line treated with doxorubicin, when coupled with IC_{20} - IC_{80} concentrations of CBD, it was evident that at higher concentrations of CBD (10 and 5 μM), there was synergy or additive effects with CI values of less than 1.1 (Table 1). The only universally antagonistic effects (CI values above 1.1) observed across the cell lines were at lower concentrations of CBD (2.5 and 1.25 $\mu\text{g/mL}$) and lower concentrations of doxorubicin suggesting that lower concentrations of both may have antagonistic effects during treatment.

When all three cell lines were treated with vincristine the 17-71 lymphoma cell line again showed to be most sensitive to the treatment with IC_{20} - IC_{80} values between 0.25 and 1 nM, while CMT12 and D17 cell lines treated with vincristine required higher concentrations to hinder cell proliferation (1.7-6.8 nM). Nearly universally, the treatment of vincristine and CBD showed synergistic or additive effects regardless of the cell line examined with nearly all CI values being 1.1 or lower, suggesting that vincristine and CBD are likely to augment the effects of one another in canine neoplastic cell lines examined (Table 1).

3.4 | Annexin V apoptosis assay

Annexin V apoptosis assays using flow cytometry were performed at 4 and 8 hours after treatment with 15 μg CBD or vehicle control

17-71					17-71				
CBD $\mu\text{g/mL}$	10	5	2.5	1.25	CBD $\mu\text{g/mL}$	10	5	2.5	1.25
Dox 0.125 μM	0.7	0.8	1.7	>2.0	Vin 1 nM	1.0	0.8	0.5	0.4
Dox 0.067 μM	0.8	1	>2.0	>2.0	Vin 0.5 nM	1.0	0.8	0.5	0.5
Dox 0.033 μM	0.7	0.8	>2.0	>2.0	Vin 0.25 nM	1.0	0.9	0.9	1.1
D17					D17				
CBD $\mu\text{g/mL}$	10	5	2.5	1.25	CBD $\mu\text{g/mL}$	10	5	2.5	1.25
Dox 2 μM	1.1	0.6	0.7	0.7	Vin 6.6 nM	1.1	0.9	1.3	0.9
Dox 1 μM	1.1	0.6	0.7	0.9	Vin 3.3 nM	0.9	0.7	1.0	1.0
Dox 0.5 μM	1.1	0.6	>2.0	>2.0	Vin 1.7 nM	0.8	0.5	0.9	0.8
CMT12					CMT12				
CBD $\mu\text{g/mL}$	10	5	2.5	1.25	CBD $\mu\text{g/mL}$	10	5	2.5	1.25
Dox 2 μM	1.0	0.6	0.5	0.5	Vin 6.6 nM	0.8	0.5	0.4	0.3
Dox 1 μM	1.0	0.7	0.8	1.1	Vin 3.3 nM	0.7	0.5	0.5	0.3
Dox 0.5 μM	1.0	0.9	1.5	1.7	Vin 1.7 nM	0.6	0.7	0.7	0.3

Note: CI values less the 0.9 suggest synergistic interactions, 0.9-1.1 suggest additive interactions and values above 1.1 suggest antagonism between the drug combination. All bolded numbers indicate additive or synergistic interactions while italicized numbers are antagonistic interactions.

TABLE 1 17-71, D17 and CMT12 cell lines CI values under dual treatment with CBD and doxorubicin (Dox) or CBD and vincristine (Vin) at various concentrations between the IC_{80} - IC_{20} concentrations for each drug combination

(methanol) for 8 hours. Annexin V staining revealed a mean percentage and SD of $31.0 \pm 10.8\%$ and $79.0 \pm 6.1\%$ positive staining cells at times 4 and 8 hours respectively in the 17-71 cell line, showing significant increases in positive cells at both 4 and 8 hours when compared with VC cells and untreated cells ($10.1 \pm 0.4\%$ and $9.9 \pm 1.2\%$, respectively). D17 cells treated with CBD showed a significant increase in Annexin V positive cells at only the 8 hours time point ($24.0 \pm 3.6\%$) when compared with VC cells ($6.5 \pm 0.6\%$) and untreated cells ($3.3 \pm 1.0\%$). D17 cells treated for

4 hours with $15 \mu\text{g}$ of CBD ($9.4 \pm 1.8\%$) were higher than VC or untreated cells, but this increase was not significant. Similarly, the CMT12 cell line showed a significant increase in positive cells at the 8 hours time point with $21.5 \pm 2.5\%$ of the cells staining for Annexin V. In the CMT12 cell line there were also increases in Annexin V stained cells ($15.7 \pm 2.2\%$) at 4 hours, but they were not significantly increased from VC treated cells ($10.9 \pm 2.0\%$) or untreated ($13.9 \pm 0.6\%$) when using nonparametric conservative statistical testing (Figure 3B).

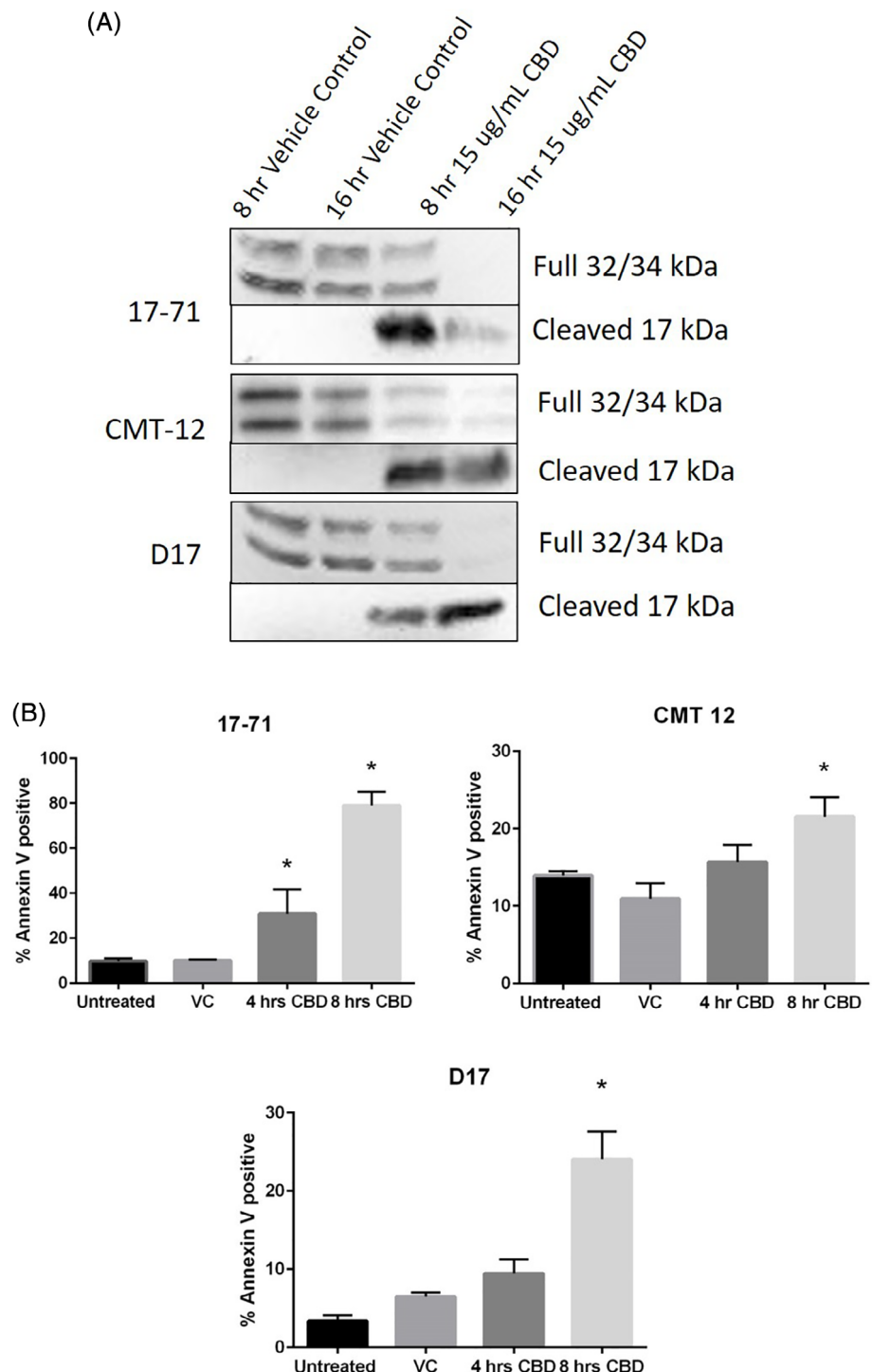


FIGURE 3 Apoptosis of neoplastic cell lines 17-71, D17 and CMT12 after treatment with $15 \mu\text{g/mL}$ of CBD. (A) Immunoblotting for cleaved caspase 3 (17 Kda) after 8 and 16 hours of CBD treatment as compared with methanol vehicle control showing cleaved caspase across all cell lines at both time points. (B) Annexin V apoptosis assay representing relative percent of Annexin V positive cells identified via flow cytometry. Mean and SD from baseline vehicle control treated cells (VC) comparing untreated and 4 and 8 hours of $15 \mu\text{g/mL}$ CBD treatment. * indicates a significant increase percentage from VC treatment ($P < .05$)

3.5 | Time course western blot analysis for pathway implications

After treatment of cells with methanol vehicle control or 10 µg/mL of CBD for 2, 4 and 8 hours numerous immunoblots were performed. The immunoblots performed using AKT and phosphorylated-AKT or mTOR and phosphorylated-mTOR showed no depression or increased intensity of the signal over time regardless of treatments over two different time course analyses experiments. The lack of changes suggest there is no alteration in the PI3Kinase-AKT-mTOR pathway as it relates to induction of autophagy or apoptosis. Assessment of the MAP kinase pathway showed repeatable increases in both ERK and JNK phosphorylation across all three cell lines in the presence of 10 µg/mL of CBD when compared with equal amounts of methanol vehicle control treatment over the 8 hour time-course (Figure 4). The presence of baseline ERK and JNK phosphorylation were not evident in 17-71 cells and both showed abundant phosphorylation peaking at 4 hours of treatment with CBD. The ERK baseline phosphorylation was more evident in D17 and CMT12 cells and was rapidly induced peaking at 2-4 hours in these cell lines (Figure 4). The JNK phosphorylation status was robust in the CMT12 cells lines after CBD treatment, while the D17 cells showed a more mild induction of phosphorylated JNK. Overall, the baseline JNK and ERK protein expression across the cell lines did not change substantially regardless of treatment or time. The blots presented are representative of duplicate time course immunoblotting experiments performed.

In tandem to these time course analyses the assessment of LC3 protein was assessed as part of the autophagy response in cells over 8 hours. Universally, in all three cell lines there was an increase in the LC3II proportion of LC3 protein which represents the ethanolamine conjugated form of the protein found in autophagy vesicles or autophagosomes. This increase in LC3II was prominent starting at 2 hours of treatment and persists throughout the 8 hours of treatment which is not observed in vehicle control treated cells. (Figure 5A). Coupled with the LC3II response one also observes a marked decrease in western blotting for the autophagy cargo carrier protein p62 which is another marker for autophagy often discussed in the literature.³⁷ These observations are also accompanied by an activation of caspase 3 which can also be seen at 2 hours in the 17-71 cells, but is not evident until hour 8 in the CMT12 and D17 CBD treated cells showing autophagy appears to precede the apoptotic response in these cells (Figure 5A).

3.6 | Immunofluorescence for LC3I/II

Cellular fluorescence imaging was captured at 400 and 600 times magnification for the D17 and CMT12 cell lines, respectively. The use of rabbit polyclonal antibody as a control showed a mild background fluorescence that is minimal with or without 10 µg/mL of CBD treatment (Figure 5B). When using the LC3A/B rabbit polyclonal antibody there was a mild diffuse cytoplasmic staining in methanol vehicle control treated cells regardless of the cell line used. In both the CMT12

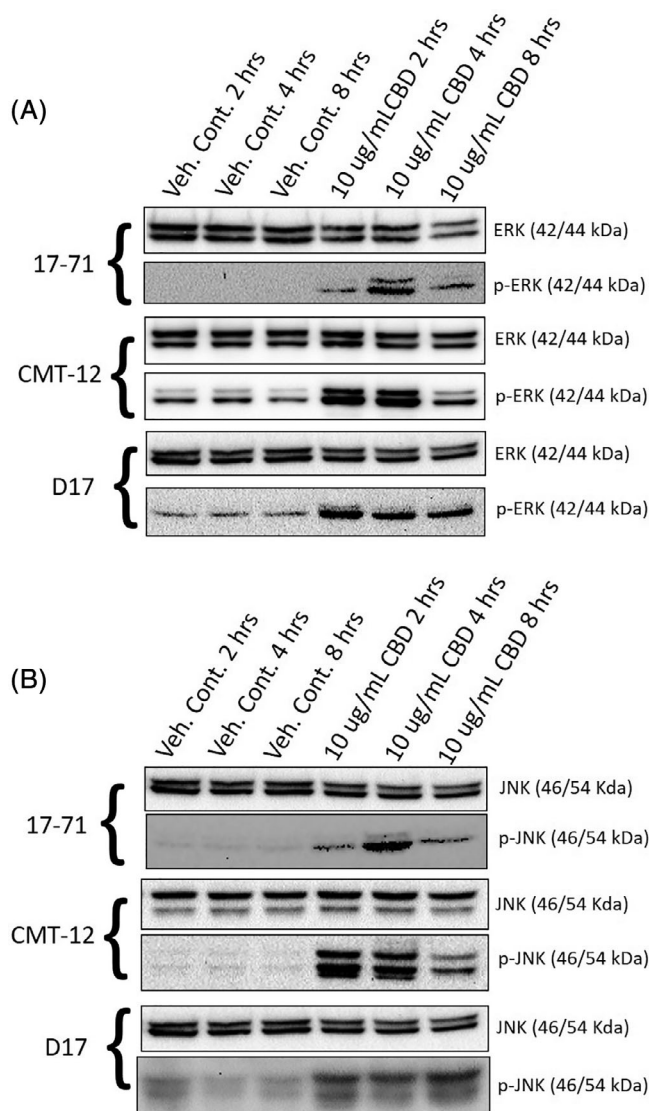


FIGURE 4 Time-course immunoblotting for phosphorylated MAP kinases in relationship to baseline protein expression with vehicle control treated or 10 µg/mL CBD. (A) ERK and phosphorylated ERK expression at time 2, 4 and 8 hours compared with methanol vehicle control treated cells showing extensive phosphorylation of 17-71, D17 and CMT12 cell lines at 2, 4 and 8 hours. (B) JNK and phosphorylated JNK expression at time 2, 4 and 8 hours compared with methanol vehicle control treated cells showing variable phosphorylation of 17-71, D17 and CMT12 cell lines at 2, 4 and 8 hours

and the D17 cells when treated with 10 µg/mL of CBD immunofluorescence with the LC3A/B antibody showed numerous discrete punctate intensely staining vesicles which are consistent with LC3 protein localization to autophagosomes or autophagolysosomes (Figure 5B).

4 | DISCUSSION

Client pursuits of complementary and/or alternative therapies following the diagnosis of cancer in their animal companions is not

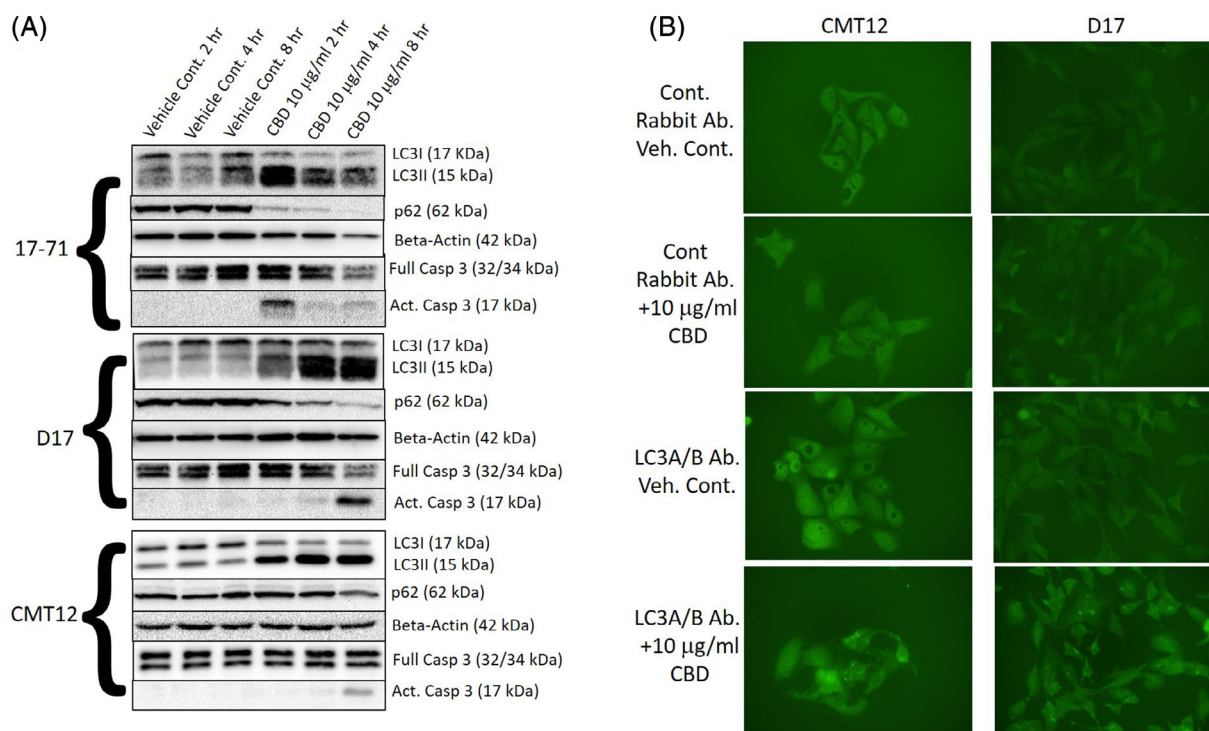


FIGURE 5 (A) Time course immunoblotting for LC3 A/B autophagy phase shift because of prenylation, p62 degradation and caspase 3 activation in 17-71, CMT12 and D17 cell lines. Cells treated for 2, 4 or 8 hours with vehicle control or 10 µg/mL CBD. LC3I to LC3II shift occurs in all three cell lines observed within 2 to 4 hours with caspase activation occurring between 2 and 8 hours suggesting autophagy precedes apoptosis. (B) Immunofluorescence for LC3A/B (6 hours of treatment). CMT12 cells (600x) and D17 (400x) cell lines depicted in columns. Control Rabbit Antibody immunostaining on vehicle control treated cells (Row 1). Control Rabbit Antibody immunostaining on CBD 10 µg/mL treated cells (Row 2). Rabbit LC3 A/B antibody immunostaining in vehicle control treated cells showing variable staining of cell cytoplasm (Row 3). Rabbit LC3A/B immunostaining in cells treated with 10 µg/mL CBD showing punctate autophagosomes in cytoplasm of cells (Row 4)

uncommon. Because of the increasing interest and availability, the use of CBD-based products in people and their pet companions is becoming quite prevalent, with cancer and quality of life during cancer treatment being a commonly reported reason for hemp related treatments in pets, regardless of doctor recommendations.³⁰ Although there are numerous cell culture reports on the cytotoxicity of cannabinoids in human cancer cell lines there are no reports available in canine cancer cell lines. CBD-induced cell death, has been well documented in murine models and human cancer cell lines from a wide range of histology.^{16,38-40} A main objective of our study was to examine whether CBD and its native acidic form (CBDA) caused similar cytotoxic effect in a select number of common canine cancers, representing mesenchymal, round, and epithelial origins. In accordance with numerous human cell lines studies, our results show that CBD resulted in similar canine cancer cell death uniformly, while CBDA has little to no effect at the concentrations used except for a mild effect on the lymphoma cell line at the highest concentrations. These assays were allowed to incubate for 48 hour similar to other natural products studied by our laboratory, which often required longer than 24 hours to induce cytotoxicity. The MTT assay used provides a limited view into the anti-proliferative/viable cell mass effects of CBD since its action is purely based on NADH ability to reduce the formazan dye in mitochondria

and CBD might have directly inhibited this reaction. However, short duration MTT assays of 6 hours using CBD with these cell lines suggests that the NADH oxidase activity is not decreased by CBD (data not shown; supplementary figure 1). Therefore, the MTT assay is sufficient to assume relative cytotoxicity regardless of CBD's ability to potentially alter mitochondrial permeability since NADH electron donation to the formazan dye should still be present in the face of permeability changes.^{41,42}

Our data demonstrates significant reductions in canine cancer cell proliferation when treated with CBD concentrations ranging from 2.5 to 10 µg/mL with similar effects on all 5 cell lines examined. Interestingly, the CBD-rich whole hemp extract used in this study resulted in a significant reduction in cancer cell proliferation at the lowest CBD concentrations, ranging from 0.67 to 10 µg/mL. When using the whole hemp extract we used CBD concentrations identical to what was used in the pure CBD experiments. The lethality of CBD in the presence of CBDA and/or other phytocannabinoids and terpenes at lower concentrations are likely what potentiated the whole plant extract effects in this study. This synergistic finding is commonly reported in as the "entourage effect", whereby the mixture of cannabinoids and terpenes work in concert to produce an augmented effect. This interplay is indeed complex, involving factors such as the

specific chemovars and the cannabimimetic receptor expression patterns of the specific cancer cell line, and recent research shows that certain hemp cultivars (or chemovars) are vastly different in their cytotoxic effects, making cannabis biology interesting for future investigations into disease specific cultivar/chemovar treatments.⁴³

The effects on cell death appear to be universal across both proliferative and normal slow growing fibroblasts. Given their slow-proliferative nature, it is unlikely that the mechanism of cell death in these cells is attributable to perturbation of proliferation pathways. Although the exact nature of this decreased viability of slow or non-proliferative cells was not explored further in this study, CBD-induced apoptosis through alterations in cellular levels of reactive oxygen species (ROS) and reductions in intracellular thiols leading to autophagy and apoptosis has been described in a number of other slow or non-proliferating cell models.⁴⁴⁻⁴⁶

The cell proliferation response of 17-71, CMT12 and D17 cell lines when treated with 10 to 15 µg/mL CBD results in apoptosis, as substantiated by Annexin V staining and cleaved caspase 3 immunoblotting, and occurs within 8 hours of treatment. In addition, an autophagic response is observed with a proportional phase shift of LC3-I to the phosphatidyl-ethanolamine LC3-II moiety of the protein, p62 degradation and localization of autophagosomes-associated LC3 proteins. In conjunction with this rise in LC3-II there is a concomitant decrease in the autophagy cargo adapter protein SQSTM1/p62. This adaptor protein is often used as a confirmatory marker of autophagy response, however nuances in its upregulation can often prove negative results and when changes are not observed other protease inhibitors or autophagy inhibitors are needed to confirm autophagy flux.^{37,47} Based on our results autophagy flux is worth further investigation utilizing such techniques across cell lines because of the differences in timing of induction with a prompt response in 17-71 cells and longer time to p62 degradation in CMT12 cells. Given this time course, the autophagy response we observe likely promotes the apoptosis response in these cell lines. CBD, as well as other cannabinoids' ability to induce autophagy is well established and further supported by our data.⁴⁸⁻⁵⁰ The underlying mechanism by which autophagy and apoptotic responses are elicited at different time points in these cell lines require future investigation and may not be ubiquitous across cancers. Further studies in canine cancer cell systems examining mitochondrial dysregulation and mitophagy could also be fruitful to better understand this autophagy response, as our focus was limited to examination on cellular signalling pathways and apoptosis induction.

Investigation into the basic cellular signalling mechanisms revealed no alterations that were pronounced in signalling pathways through AKT or mTOR signalling. However, there was a repeatable and dramatic rise in the phosphorylation of MAP kinase pathways, in particular ERK and JNK signalling, with minimal influence on the p38 phosphorylation and activation. Prior studies have implicated perturbation of major MAP kinase pathways, observed by alterations in ERK and JNK phosphorylation in human melanoma, colon, ovarian, thyroid and leukaemia cancer cell lines.⁵¹⁻⁵⁵ ERK phosphorylation is often implicated as a cellular growth and survival pathway, while JNK has been implicated in cellular stress and induction of apoptosis and

potentially even autophagy.⁵⁶ The exact receptor activation leading to these events are likely through the poorly defined orphan G protein receptor pathways which have been implicated in CBD signalling and further study in this area is warranted to better understand the juxtaposition of ERK and JNK dual activation with CBD treatment.

Most importantly to the clinical oncology community is the documented synergistic and antagonistic results on cancer cell proliferation when canine cancer cells were treated with commonly utilized chemotherapeutics in combination with CBD. The combination of vincristine and CBD consistently potentiated the decrease in cell viability as compared with either treatment alone proving that at lethal to sublethal dosing of both CBD and vincristine there is a prominent synergistic response. Interestingly, combination treatment of doxorubicin and CBD resulted in both synergistic and antagonistic outcomes depending on the specific concentrations of each compound used. Based on our results it appears that as more lethal doses of CBD and doxorubicin are utilized there is an additive to synergistic response, while at sublethal dosing the effect may be antagonistic. The doses of doxorubicin used in these in-vitro assays was at the higher end of what is observed in serum of dogs during IV infusion when treating the CMT12 and D17 cell lines (1-2 µM) while the 17-71 cell line was far more sensitive to doxorubicin treatment at nearly 1/10th the concentration.⁵⁷ Similarly, the 17-71 cell line was more sensitive to vincristine than the D17 and CMT12 cell lines and all of the concentrations used were at 5-20-fold lower than what has been observed to be effective in canine clinical use which is approximately 20 to 40 nM.^{58,59} Exactly how these in-vitro incubations with the chemotherapies translate into physiologically achievable transient concentrations is surely speculation, but we appear to be at physiologically achievable concentrations of these chemotherapies. Unfortunately, the CBD concentrations necessary to induce cytotoxicity are relatively high and likely not physiologically achievable (>1 µg/mL); as the highest concentrations to date using 20 mg/kg body weight orally twice a day could only achieve approximately 0.7 µg/mL at a steady state in the bloodstream of dogs.⁶⁰ This finding is of critical clinical importance as many clients are concurrently providing CBD with chemotherapy at far lower concentrations than what we find to be effective on cell proliferation, but the exact effects of this lower dosing may alter cytochrome p450 metabolism and has the potential to affect chemotherapeutic dosing.⁶¹ Currently, there is little to no information regarding doxorubicin or vincristine clinical application and how CBD co-administration during chemotherapy affects serum concentrations or chemotherapy efficacy which is sorely needed to safely administer CBD during treatment as CBD is known to affect many other pharmacologics.⁶² In dogs, this information is paramount as dogs appear to metabolize CBD differently than rodents and humans suggesting that results could be different across species.^{63,64}

As previously discussed, CBD has been shown to result in cytotoxic autophagy, but in certain instances, CBD may prompt cytoprotective autophagy through the attenuation of oxidative stress and prevention of JNK/MAPK activation.⁶⁵ Herein, we have identified that the cellular effects resulting from CBD treatment, as it relates to

the induction of autophagy and apoptosis may be related to the activation of the MAP kinase pathway as demonstrated by the prompt induction of ERK and JNK phosphorylation with autophagy. CBD has been shown to be a potent redox modulator, increasing intracellular levels of ROS.^{66,67} In accordance with our results, ROS-induced JNK and ERK activation has been implicated in the induction of both autophagy and apoptosis concurrently.⁶⁸ JNK is thought to regulate autophagy by a number of mechanisms with the role of JNK signalling and expression of autophagy-related genes (ATG) being a leading theory.⁵⁶ To the authors knowledge, the relationship between MAP kinase signalling, specifically JNK signalling, and the classically associated autophagy regulatory pathways, that is, mTOR and PI3K/Akt, has yet to be described and warrants further research, however we could show no apparent alteration in AKT signalling or mTOR signalling when performing western blots. In addition, since CBD does not affect CB1 or CB2 receptor signalling, which is a primary means of THC stimulation of cancer cells, the prompt signalling effects observed in these cell lines implicates other orphan G protein receptors such as GPCR 18 and GPCR 55 as potential targets and have yet to be interrogated in canine cancer cells regarding their presence or involvement.

In conclusion, this study demonstrated the in vitro anti-neoplastic properties of CBD on five canine cancer cell lines representative of all three major cancer lineages when used as a single agent, as well as in combination with commonly utilized chemotherapeutics. Our results are in accordance with other cannabinoid based research and offers initial insights into this field of research in veterinary medicine. Pending additional research, CBD and other cannabinoids may be utilized as adjuvant therapy for canine cancer patients, but must take into account the current chemotherapeutic protocol with trepidation because of potential drug-drug interactions. Further research into cellular signalling and receptor biology implicated by MAP kinase signalling with CBD treatment is essential to understand how CBD cytotoxic responses may lead to other chemotherapeutic synergies that utilize MAP kinase inhibitors and common chemotherapeutics for enhanced therapeutic responses.

DATA AVAILABILITY STATEMENT

The data that support the findings of this study are available from the corresponding author upon reasonable request.

ORCID

Joseph J. Wakshlag  <https://orcid.org/0000-0003-4397-6081>

REFERENCES

- Amar MB. Cannabinoids in medicine: a review of their therapeutic potential. *J Ethnopharmacol*. 2006;105(1–2):1–25.
- Gaoni Y, Mechoulam R. Isolation, structure, and partial synthesis of an active constituent of hashish. *J Am Chem Soc*. 1964;86(8):1646–1647.
- Matsuda LA, Lolait SJ, Brownstein MJ, Young AC, Bonner TI. Structure of a cannabinoid receptor and functional expression of the cloned cDNA. *Nature*. 1990;346:561–564.
- Munro S, Thomas KL, Abu-Shaar M. Molecular characterization of a peripheral receptor for cannabinoids. *Nature*. 1993;365:61–65.
- DeVane WA, Hanus L, Breuer A, et al. Isolation and structure of a brain constituent that binds to the cannabinoid receptor. *Science*. 1992;258:1946–1949.
- Mechoulam R, Ben-Shabat S, Hanus L, et al. Identification of an endogenous 2-monoglyceride, present in canine gut, that binds to cannabinoid receptors. *Biochem Pharmacol*. 1995;50(1):83–90.
- Sugiura T, Kondo S, Sukagawa A, et al. 2-Arachidonoylglycerol: a possible endogenous cannabinoid receptor ligand in brain. *Biochem Biophys Res Commun*. 1995;215(1):89–97.
- O'Sullivan SE, Kendall DA. Cannabinoid activation of peroxisome proliferator-activated receptors: potential for modulation of inflammatory disease. *Immunobiology*. 2010;215(8):611–616.
- Pertwee RG, Howlett AC, Abood ME, et al. International union of basic and clinical pharmacology. LXXIX. Cannabinoid receptors and their ligands: beyond CB1 and CB2. *Pharmacol Rev*. 2010;62(4):588–631.
- Meiri E, Jhangiani J, Vredenburg JJ, et al. Efficacy of dronabinol alone and in combination with ondansetron versus ondansetron alone for delayed chemotherapy-induced nausea and vomiting. *Curr Med Res Opin*. 2007;23(3):533–543.
- Gonzalez-Rosales F, Walsh D. Intractable nausea and vomiting due to gastrointestinal mucosal metastases relieved by tetrahydrocannabinol (dronabinol). *J Pain Symptom Manage*. 1997;14(5):311–314.
- May MB, Glode AE. Dronabinol for chemotherapy-induced nausea and vomiting unresponsive to antiemetics. *Cancer Manag Res*. 2016;8:49–55.
- Sanchez C, de Ceballos ML, Gomez del Pulgar T, et al. Inhibition of glioma growth in vivo by selective activation of the CB(2) cannabinoid receptor. *Cancer Res*. 2001;61(15):5784–5789.
- Scott KA, Dalgleish AG, Liu WM. The combination of cannabidiol and Δ^9 -tetrahydrocannabinol enhances the anticancer effects of radiation in an orthotopic murine glioma model. *Mol Cancer Ther*. 2014;13(12):2955–2967.
- Deng L, Ng L, Ozawa T, Stella N. Quantitative analysis of synergistic responses between cannabidiol and DNA-damaging agents on the proliferation and viability of glioblastoma and neural progenitor cells in culture. *J Pharmacol Exp Ther*. 2017;360(1):215–224.
- De Petrocellis L, Ligresti A, Schiano Moriello A, et al. Non-THC cannabinoids counteract prostate carcinoma growth in vitro and in vivo: pro-apoptotic effects and underlying mechanisms. *Br J Pharmacol*. 2012;168:79–102.
- Brown AJ, Hiley CR. Is GPR55 an anandamide receptor? *Vitam Horm*. 2009;81:111–137.
- De Petrocellis L, Di Marzo V. Non-CB1, non-CB2 receptors for endocannabinoids, plant cannabinoids, and synthetic cannabimimetics: focus on G-protein-coupled receptors and transient receptor potential channels. *J Neuroimmune Pharmacol*. 2010;5(1):103–121.
- Ross RA. The enigmatic pharmacology of GPR55. *Trends Pharmacol Sci*. 2009;30(3):156–163.
- Console-Bram L, Brailou E, Brailou GC, Sharir H, Abood ME. Activation of GPR18 by cannabinoid compounds: a tale of biased agonism. *Br J Pharmacol*. 2014;171(16):3908–3917.
- Marcu JP, Christian RT, Lau D, et al. Cannabidiol enhances the inhibitory effect of Δ^9 -tetrahydrocannabinol on human glioblastoma cell proliferation and survival. *Mol Cancer Ther*. 2010;9(1):180–189.
- Sultan AS, Marie MA, Sheweita SA. Novel mechanism of cannabidiol-induced apoptosis in breast cancer cell lines. *Breast*. 2018;41:34–41.
- Galve-Roperh I, Sanchez C, Cortes MI, Gomez et al. anti-tumoral action of cannabinoids: involvement of sustained ceramide accumulation and extracellular signal-induced apoptosis. *Biochem J*. 2002;6:313–319.
- Powles T, te Poele R, Shamash J, et al. Cannabis-induced cytotoxicity in leukemic cell lines: the role of the cannabinoid receptors and the MAPK pathway. *Blood*. 2005;105:1214–1221.

25. Ellert-Maklaszewska A, Kaminsha B, Konarska L. Cannabinoids down-regulate PI3K/Akt and Erk signaling pathways and activate proapoptotic function of bad protein. *Cell Signal*. 2005;17:25-37.
26. Sarker KP, Biswas KK, Yamakuchi M, et al. ASK1-p38 MAPK/JNK signaling cascade mediates anandamide-induced PC12 cell death. *J Neurochem*. 2003;85:50-61.
27. Russo EB. Taming THC: potential cannabis synergy and phytocannabinoid-terpenoid entourage effects. *Brit J Pharmacol*. 2011;163(7):1344-1364.
28. Blasco-Benito S, Seigo-Vila M, Caro-Villalobos M, et al. Appraising the "entourage effect": antitumor action of a pure cannabinoid versus a botanical drug preparation in preclinical models of breast cancer. *Biochem Pharmacol*. 2018;157:285-293.
29. Ben-Shabat S, Fride E, Sheskin T, et al. An entourage effect: inactive endogenous fatty acid glycerol esters enhance 2-arachidonoyl-glycerol cannabinoid activity. *Eur J Pharmacol*. 1998;353:21-31.
30. Kogan LR, Hellyer PW, Robinson NG. Consumers' perceptions of hemp products for animals. *J Am Holist Vet Med Assoc*. 2016;42:40-48.
31. Vega-Avila E, Pugsley MK. An overview of colorimetric assay methods used to assess survival or proliferation of mammalian cells. *Proc West Pharmacol Soc*. 2011;54:10-14.
32. Chou TC. Drug combination studies and their synergy quantification using the Chou-Talalay method. *Cancer Res*. 2010;70(2):440-446.
33. Syrjä P, Anwar T, Jokinen T, et al. Basal autophagy is altered in Lagotto Romagnolo dogs with an ATG4D mutation. *Vet Pathol*. 2017;54(6):953-963.
34. Gordon IK, Ye F, Kent M. Evaluation of the mammalian target of rapamycin pathway and the effect of rapamycin on target expression and cellular proliferation in osteosarcoma cells from dogs. *Amer J Vet Res*. 2008;69:1079-1084.
35. Ikari A, Atomi K, Kinjo Y, Sugatani J. Magnesium deprivation inhibits a MEK-ERK cascade and cell proliferation in epithelial Madin-Darby canine kidney cells. *Life Sci*. 2010;86:766-773.
36. Levine CB, Bayle J, Biourge V, Wakshlag JJ. Effects and synergy of feed ingredients on canine neoplastic cell proliferation. *BMC Vet Res*. 2016;12(1):159.
37. Yoshi SR, Mizushima N. Monitoring and measuring autophagy. *Int J Mol Sci*. 2017;18:1865.
38. Solina M, Massi P, Cinquina V, et al. Cannabidiol, a non-psychoactive cannabinoid compound, inhibits proliferation and invasion in U87-MG and T98G glioma cells through a multitarget effect. *PLoS One*. 2013;8(10):e76918.
39. McKallip RJ, Jia W, Schlomer J, et al. Cannabidiol-induced apoptosis in human leukemia cells: a novel role of cannabidiol in the regulation of p22^{phox} and Nox4 expression. *Mol Pharmacol*. 2006;70(3):897-908.
40. Ligresti A, Moriello AS, Starowicz K, et al. Antitumor activity of plant cannabinoids with emphasis on the effect of cannabidiol on human breast carcinoma. *J Pharmacol Exp Ther*. 2006;318(3):1375-1387.
41. Kuman P, Nagarahan A, Uchil PD. Analysis of cell viability by the MTT assay. *Cold Spring Harb Protoc*. 2018;469-471.
42. Riss TL, Moravec RA, Niles AL, et al. Cell viability assays. In: Markossian S, Sittampalam GS, Grossman A, et al., eds. *Assay Guidance Manual*. Bethesda, MD: Eli Lilly & Company and the National Center for Advancing Translational Sciences; 2016 <https://www.ncbi.nlm.nih.gov/books/NBK144065/>.
43. Baram L, Peled E, Berman P, et al. The heterogeneity and complexity of Cannabis extracts as antitumor agents. *Oncotarget*. 2019;10(41):4091-4106.
44. Wu HS, Chu RM, Wang CC, et al. Cannabidiol-induced apoptosis in primary lymphocytes is associated with oxidative stress-dependent activation of caspase-8. *Toxicol Appl Pharmacol*. 2008;226(3):260-270.
45. Lee CY, Wey SP, Liao MH, Hsu WL, Wu HY, Jan TR. A comparative study on cannabidiol-induced apoptosis in murine thymocytes and EL-4 thymoma cells. *Int Immunopharmacol*. 2008;8(5):732-740.
46. Wu HY, Chang AC, Wang CC, et al. Cannabidiol induced contrasting pro-apoptotic effect between freshly isolated and precultured human monocytes. *Toxicol Appl Pharmacol*. 2010;246(3):141-147.
47. Klionsky D, Abdelmohsen K, Abe A, et al. Guidelines for the use and interpretation of assays for monitoring autophagy (3rd edition). *Autophagy*. 2016;12(1):1-222.
48. Shrivastava A, Kuzontkoski PM, Groopman JE, Prasad A. Cannabidiol induced programmed cell death in breast cancer cells by coordinating the cross-talk between apoptosis and autophagy. *Mol Cancer Ther*. 2011;10(7):1161-1172.
49. Nabissi M, Morelli MB, Amantini C, et al. Cannabidiol stimulates Aml-1a-dependent glial differentiation and inhibits glioma stem-like cells proliferation by inducing autophagy in a TRPV2-dependent manner. *Int J Cancer*. 2015;137(8):1855-1869.
50. Costa L, Amaral C, Teixeira N, Correia-da-Silva G, Fonseca BM. Cannabinoid-induced autophagy: protective or death role? *Prostag Oth Lipid Met*. 2016;122:54-63.
51. Satyamoorthy K, Li G, Guerrero MR, et al. Constitutive mitogen-activated protein kinase activation in melanoma is mediated by both BRAF mutations and autocrine growth factor stimulation. *Cancer Res*. 2003;63(4):756-759.
52. Bos JL, Fearson ER, Hamilton SR, et al. Prevalence of ras gene mutations in human colorectal cancers. *Nature*. 1987;327:293-297.
53. Steinmetz R, Wagoner HA, Zeng P, et al. Mechanisms regulating the constitutive activation of the extracellular signal-regulated kinase (ERK) signaling pathway in ovarian cancer and the effect of ribonucleic acid interference for ERK1/2 on cancer cell proliferation. *Mol Endocrinol*. 2004;18(10):2570-2582.
54. Piscazzi A, Costantini E, Maddalena F, et al. Activation of the RAS/-RAF/ERK signaling pathway contributes to resistance to Sunitinib in thyroid carcinoma cell lines. *J Clin Endocrinol Metab*. 2012;97(6):E898-E906.
55. Towatari M, Iida H, Tanimoto M, Iwata H, Hamaguchi M, Saito H. Constitutive activation of mitogen-activated protein kinase pathway in acute leukemia cells. *Leukemia*. 1997;11(4):479-484.
56. Zhou Y-Y, Li Y, Jiang W-Q, Zhou L-F. MAPK/JNK signaling: a potential autophagy regulation pathway. *Biosci Rep*. 2015;35(3):e00199.
57. Gustafson DL, Rastatter JC, Colombo T, Long ME. Doxorubicin pharmacokinetics: macromolecule binding, metabolism, and excretion in the context of a physiologic model. *J Pharm Sci*. 2002;91:1488-1501.
58. Xiong J, Mao W, Shi R, et al. Pharmacokinetics of liposomal-encapsulated and un-encapsulated vincristine after injection of liposomal vincristine sulfate in beagle dogs. *Cancer Chemother Pharmacol*. 2014;73:459-466.
59. Hantrakul S, Klangkaew N, Kunakornsawat S, et al. Clinical pharmacokinetics and effects of vincristine sulfate in dogs with transmissible venereal tumor (TVT). *J Vet Med Sci*. 2014;76(12):1549-1553.
60. Bartner LR, McGrath S, Rao S, Hyatt LK, Wittenburg LA. Pharmacokinetics of cannabidiol administered by 3 delivery methods at 2 different dosages to healthy dogs. *Can J Vet Res*. 2018;82(3):178-183.
61. Zendulka O, Dovrtelova G, Noskova K, et al. Cannabinoids and cytochrome P450 interactions. *Curr Drug Metab*. 2016;17:206-226.
62. Brown JD, Weinterstein AG. Potential adverse drug events and drug-drug interactions with medical and consumer cannabidiol (CBD) use. *J Clin Forensic Med*. 2019;8(989):1-24.
63. Harvey DJ, Samara E, Mechoulam R. Comparative metabolism of cannabidiol in dog, rat and man. *Pharmacol Biochem Behav*. 1991;40(3):523-532.
64. Wakshlag JJ, Schwark WS, Deabold KA, et al. Pharmacokinetics of cannabidiol, cannabidiolic acid, Δ^9 -tetrahydrocannabinol, tetrahydrocannabinolic acid and related metabolites in canine serum after dosing with three oral forms of hemp extract. *Front Vet Sci*. 2020;7:505.

65. Yang L, Rozenfeld R, Wu D, Devi LA, Zhang Z, Cederbaum A. Cannabidiol protects liver from binge alcohol-induced steatosis by mechanisms including inhibition of oxidative stress and increase in autophagy. *Free Radical Bio Med*. 2014;68:260-267.
66. Booz GW. Cannabidiol as an emergent therapeutic strategy for lessening the impact of inflammation on oxidative stress. *Free Radical Bio Med*. 2011;51(5):1054-1061.
67. Massi P, Vaccani A, Bianchessi S, Costa B, Macchi P, Parolaro D. The non-psychoactive cannabidiol triggers caspase activation and oxidative stress in human glioma cells. *Cell Mol Life Sci*. 2006;63:2057-2066.
68. Wong CH, Iskandar KB, Yadav SK, Hirpara JL, Loh T, Pervaiz S. Simultaneous induction of non-canonical autophagy and apoptosis in cancer cells by ROS-dependent ERK and JNK activation. *PLoS One*. 2010;5(4):e9996.

SUPPORTING INFORMATION

Additional supporting information may be found online in the Supporting Information section at the end of this article.

How to cite this article: Henry JG, Shoemaker G, Prieto JM, Hannon MB, Wakshlag JJ. The effect of cannabidiol on canine neoplastic cell proliferation and mitogen-activated protein kinase activation during autophagy and apoptosis. *Vet Comp Oncol*. 2020:e12669. <https://doi.org/10.1111/vco.12669>